



Quality improvement and mode evolution of high-Q lithium niobate micro-disk induced by “light annealing”

LICHENG GE,¹ HAOWEI JIANG,¹ YI'AN LIU,¹ BING ZHU,¹ CHENGHAO LU,¹ YUPING CHEN,^{1,*} AND XIANFENG CHEN¹

¹State Key Laboratory of Advanced Optical Communication Systems and Networks, School of Physics and Astronomy, Shanghai Jiao Tong University, 800 Dongchuan Road, Shanghai 200240, China

*ypchen@sjtu.edu.cn

Abstract: High-quality factor microresonators are a key component in photonic integrated circuits. However, it is more difficult to precisely engineer a single component after fabrication as integration density gets higher. In this work, we improve the quality factor of the fabricated resonator by femtosecond laser shots. The high repetition laser pulses scatter into the cavity, and then the localized high-density light field introduces a light refining and “annealing” process that may restore the lattice disorders. The intrinsic quality factor of a measured mode can be promoted from 2.17×10^5 to 1.84×10^6 . Moreover, increasing the shot power may kill the high order modes, and only the fundamental mode survives. This method may inspire new potential application in femtosecond laser modification in photonic integrated circuits.

© 2019 Optical Society of America under the terms of the [OSA Open Access Publishing Agreement](#)

1. Introduction

Lithium niobate crystal offers attractive properties such as electro-optic, nonlinear optical and acousto-optic effects in a wide wavelength range so that it is awarded as “photonic silicon”. The commercialization of lithium niobate on insulator (LNOI) is revolutionizing the lithium niobate industry [1], calling significant interest in the platform for photonic integrated circuits on a single chip [2]. LNOI has excellent properties as bulk LN and offers stronger optical confinement and a high optical element integration density which has made success in silicon on insulator (SOI) platform. As chip components, optical waveguide [3], wavelength converter [4–6], electro-optic modulator [7, 8] and resonant structures [9, 10] are all intensively studied in the past few years. Here we focus on whispering gallery mode (WGM) micro-disk resonators. It confines light at the edge of the resonator via total internal reflection leading to remarkably high intra-cavity optical intensities. It has attracted much attention also due to the combination of high quality factor, tunable coupling features and fruitful applications [11, 12]. Since LN is perceived as a difficult-to-etch material [13], the fabrication of high quality (Q) micro-disk has been intensively studied. The first LN micro-disk was fabricated using selective ion implantation combined with chemical etching and thermal treatment [9]. After the commercialization of LN thin film, fabrication utilizing electron beam lithography and photolithography has taken the dominant position [14, 15] enabling mass production and being cost effective. A more flexible method combining femtosecond laser writing and focused ion beam (FIB) milling has been proposed which is more powerful and convenient to engineer single micro-disk [16].

However, we often come into some situations that after resonator fabrication or even it is integrated to other building blocks on a chip we need to further engineer it due to contamination in the lab or multi-time measurement. People find that clean surface and smooth sidewall are the most important two factors to achieve high Q-factor resonators [17]. In this way, many proposals have been tried. A selective reflow process utilizing CO₂ laser illumination was applied to get silica microtoroid with Q-factor in excess of 100 million [18]. A multipass exposure process

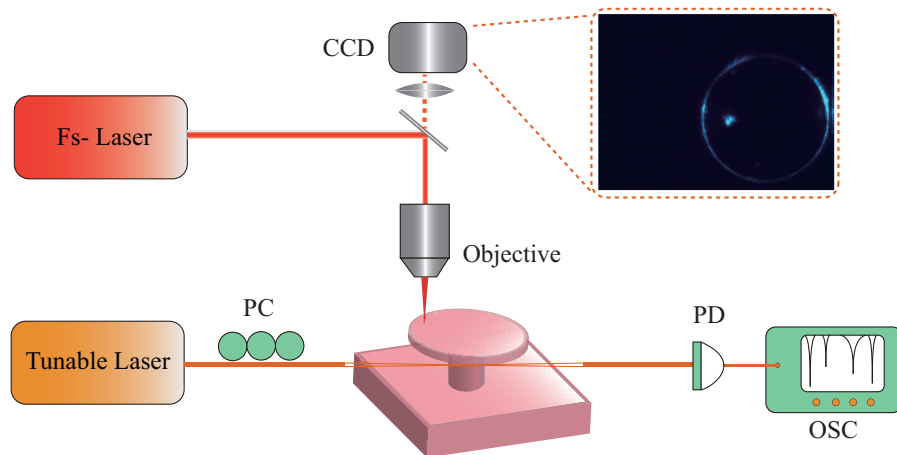


Fig. 1. Experimental setup of the dual-beam pump-probe system. The inset shows the optical image of interaction between femtosecond laser and LN micro-disk. PC: polarization controller. PD: photo detector. OSC: oscilloscope.

in electron beam lithography combined with SiO_2 cladding can help improve optical Q-factor to over 10^7 for a LN microring resonator [19]. In the most recent studies a chemo-mechanical polishing process was applied and the quality factors can be further improved [20]. All of these methods are focused on ameliorating the fabrication process to improve the Q-factor. Here we present a solution that using focused femtosecond laser can precisely repair or refine the micro-disk after fabrication. A tiny defect on the surface will scatter the laser pulses into cavity modes and induce "light annealing" process to further smooth the periphery of the micro-disk. The Q factor can have one order of magnitude increment in our demonstration. As far as we know, it is the first time that after integration the Q factor of the micro-disk can be further improved.

2. Experimental setup

Experimental setup is shown in Fig.1. The light from C-band tunable laser shown in orange lines in Fig.1) serves as probe light and passes through a polarization controller in order to control the polarization state. A silica tapered fiber is used as a local evanescent probe to couple the continuous C-band laser into and out of the micro-disk resonator. The spectrum of the output light is measured by oscilloscope (OSC). A femtosecond laser (shown in red lines in Fig.1) which plays the role of interacting wave goes through a micromachining system and is focused on the surface of the LN micro-disk via a $100\times$ microscope objective (NA=0.9). The focusing spot is about $1\mu\text{m}$ in diameter. The sample is put on a precision XYZ piezo-stage which is used to control the distance between micro-disk and tapered fiber. Both of them are placed on the moving stage of the micromachining system. The inset shows the optical image when femtosecond laser is shot on the micro-disk.

We fabricated the micro-disk using a FIB assisted femtosecond laser direct writing method [16]. First we used femtosecond laser to inscribe the prototype on a Z-cut 600nm LNOI (from NANOLN) and then FIB was applied to polish the periphery. The silica layer underneath the disk is partially removed by hydrofluoric etching, only leaving a silica pedestal in the disk center behind. After fabrication we put the sample on the stage and carefully move the tapered fiber close to it. The distance between the taper and the micro-disk is kept the same for each measurement. Then we turn on the femtosecond laser and focus it on the surface of the micro-disk. The laser is centered at 1030nm with a pulse width of 600fs and the repetition rate is set to be 300kHz. The

focusing spot is chosen to be in the middle of the periphery and the center [21, 22]. Only a small focusing spot can be seen when the laser power is under threshold. After 10^4 pulses we shut down the femtosecond laser and measure the transmission spectra. Then we raise up the laser power and do the measurement again. We can clearly see the light is scattered into the cavity and confined in the periphery as shown in the inset in Fig.1. When we shut down the laser a hardly visible defect can be found on the surface. It helps the laser scatter into cavity and the pulses will either circulate around the periphery through chaos-assisted coupling or be directly transmitted to the edge. As the laser power goes up more light will be scattered into the disk and the periphery will be brighter.

3. Results and discussion

First we characterize the micro-disk before femtosecond laser irradiation. Fig.2(a) shows the original transmission spectrum. From the spectrum different sets of high Q resonant modes are identified and marked with different color labels, showing a similar free spectral range (FSR) about 6.2nm. In order to analyze the impact of femtosecond laser interaction we focus on the high Q modes marked as mode 1, 2 and 3 corresponding to $TE_{2,260}$, $TM_{3,267}$ and $TE_{1,251}$, respectively. The detailed spectra with Lorentzian fits show high intrinsic Qs of 2.65×10^5 , 3.00×10^5 and 2.17×10^5 for mode 1, 2 and 3 respectively. We choose these three modes for two reasons. On one hand these three modes have different radial mode numbers which opens a window to investigate

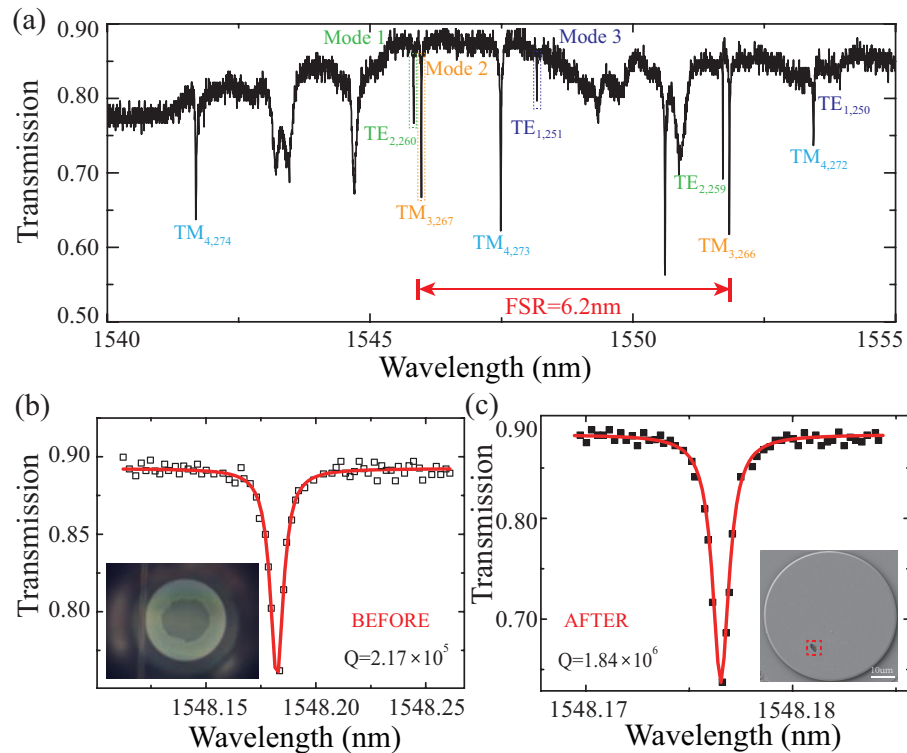


Fig. 2. (a) Transmission spectrum of the original LN micro-disk resonator with a diameter of $55 \mu\text{m}$. (b) and (c) shows Lorentzian fit of mode 3 around 1548.18 nm before and after laser interaction, respectively. The intrinsic Q has one order of magnitude promotion from 10^5 to 10^6 . The inset in (b) shows the original coupled micro-disk. The inset in (c) exhibits SEM image of the disk after femtosecond laser shots.

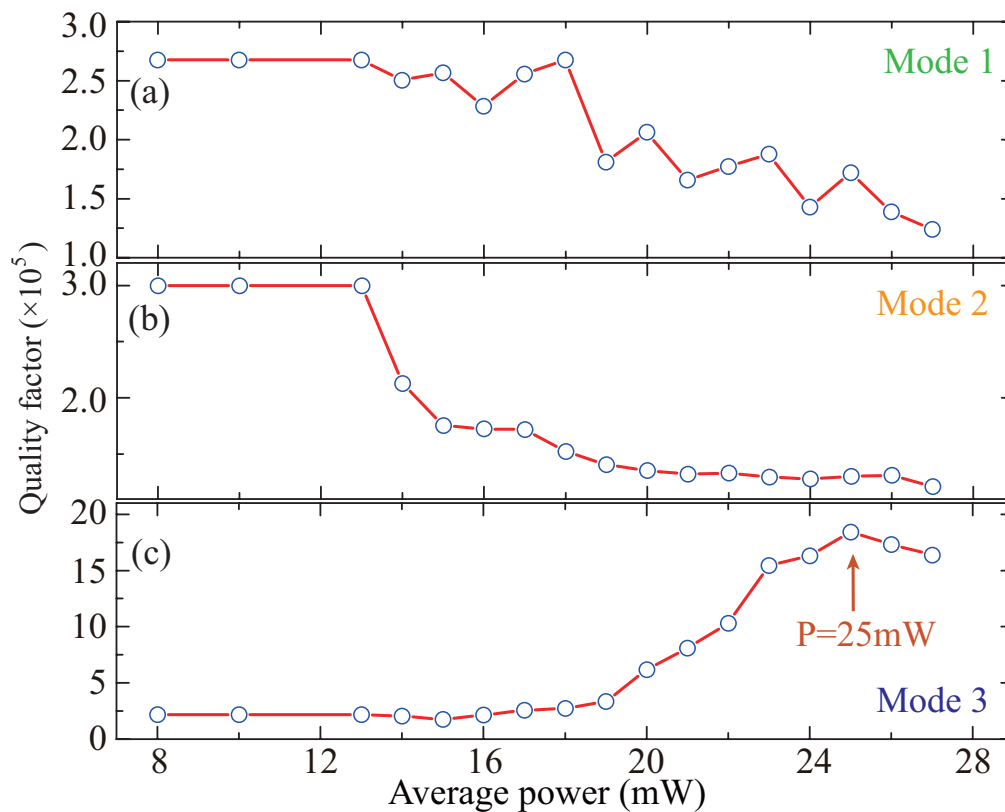


Fig. 3. The relationship between Q factors and interacting laser power. (a) (b) and (c) correspond to mode 1, 2 and 3 respectively.

the laser influence on the modes belonging to different mode families. On the other hand they are in one FSR which reduces other secondary influence factors. After femtosecond laser interaction we find it very interesting that the Q factor of mode 3 will experience an increase. Fig. 2 (b) shows the magnified spectra of mode 3 before femtosecond laser interaction while Fig. 2 (c) shows the Lorentzian fit of mode 3 after 25mW laser interaction. The intrinsic Q is calculated to be 1.84×10^6 , which has one order of magnitude increment compared with the original one. The inset shows the defect created by femtosecond laser on LN disk surface.

We also inspect mode 1 and 2 after femtosecond laser interaction. Fig. 3 shows the relationships between the measured Q factors of all the three modes and the interacting femtosecond laser power. When the laser power is under threshold, it doesn't make any change on the micro-disk so that the Q factors of all the three modes keep the same. As soon as the laser power reaches optical damage threshold of LN, it forms a tiny defect on the surface and the Q factors start to change. From Fig. 3 we can see that the Q factors of mode 1 and 2 both experience a small drop. However the evolution process of the two modes exhibits some differences. In the process of decline, mode 1 experiences some oscillation while mode 2 shows a relatively smooth drop. To the contrary mode 3 experiences a Q increment for about one order of magnitude.

For better understanding of the mode evolution process, we first compare the surface roughness of the disk before and after laser interaction. We did AFM (Dimension ICON, Bruker) measurement on the other microdisk right after its fabrication. The AFM probe is silicon tip with Al coating, the tip radius is 2nm. The cantilever stiffness k equals to 0.4N/m, and resonance frequency f_0 equals to 70kHz. The disk has the same size as the original one and possesses Q

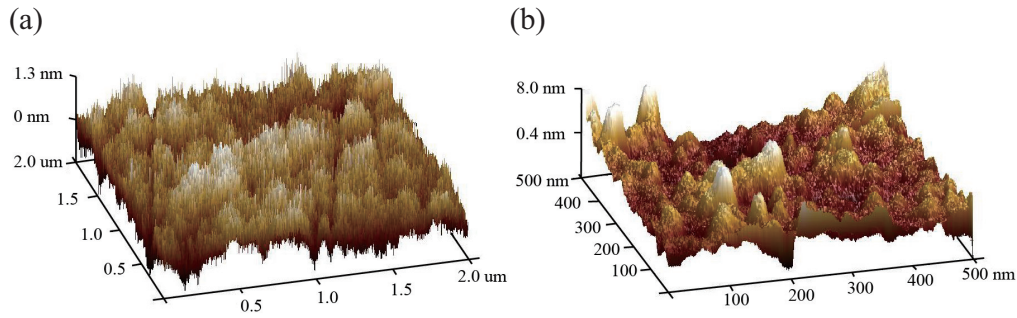


Fig. 4. Surface roughness (a) before and (b) after femtosecond laser shotting. There exist many nano particles around the hole after post-fabrication in (b).

factor of 10^5 . Fig.4 (a) is the AFM image of the original LN disk surface. We scanned a $2\mu\text{m} \times 2\mu\text{m}$ area. Then we did the post-fabrication process with 25mW femtosecond laser irradiation. Another AFM test was performed to re-check the surface roughness after the hole formation. Fig.4 (b) shows the AFM image after laser interaction. The scanning area is $0.5\mu\text{m} \times 0.5\mu\text{m}$ and is about $5\mu\text{m}$ away from the hole boundary. We can find that around the hole there exist particles about tens of nanometer wide and a few nanometer high. The surface cleanliness is obviously decreased and this will contribute to a Q degradation. The hole itself also has some impacts on the modes. We simulated intensity distribution in the radial direction of the three mode as shown in Fig.5. Mode 2 ($n=3$) extends the most about $9\mu\text{m}$ into the interior from the periphery of the disk while mode 1 ($n=2$) and 3 ($n=1$) only extends $7.5\mu\text{m}$ and $5\mu\text{m}$. The orange zone in Fig.5 represents the heat affected zone (HAZ) of the femtosecond laser. HAZ is the area of base material which is not ablated or melted by the laser irradiation but has had its micro structure, properties and refractive index altered. The 2-D thermal diffusion length of laser pulses determines the area of HAZ. It can be obtained from [23]

$$L_D = \sqrt{4 \frac{D}{R_P}}. \quad (1)$$

where L_D is the thermal diffusion length, $D=1.7 \times 10^{-3} \text{ cm}^2/\text{s}$ is the thermal diffusivity of LN. R_P is the repetition rate of the laser pulses. Through calculation we find that the HAZ extends about $1.5\mu\text{m}$ away from the hole boundary. From the figure we can see the HAZ of the laser has some overlapping with the intensity distribution of mode 2 in the radial direction. It will certainly decrease the Q since the refractive index and micro structure of HAZ is altered. Another effect we suppose is that the defect will help the laser scatter into the cavity [24–26] and induce "light annealing" process. Since the laser has high repetition rates and peak power, it reaches the periphery of the disk and will have some physical effects on the LN lattices [23]. The nonlinear absorption of the laser radiation will result in the formation of ultra-fast electron-hole plasma confined in the solid. Energy will be transferred to lattice via electron-phonon coupling, provoking a temperature increase and local melting [27]. Some lattice disorders and tiny burrs on the periphery will be repaired by the laser induced resolidification process after irradiation [28–30]. In this way the Q factor will experience an increase after laser interaction.

From above analysis we can understand different actions of the three modes. The Q factor of mode 1 have some oscillation during the drop because the invisible debris and "light annealing" process competes in the time of the laser interaction. When debris effect takes the dominant position, the Q will decrease. On the contrary when "light annealing" process is in charge it will show an increase. Mode 2 experiences a relatively smooth drop because it is mostly affected

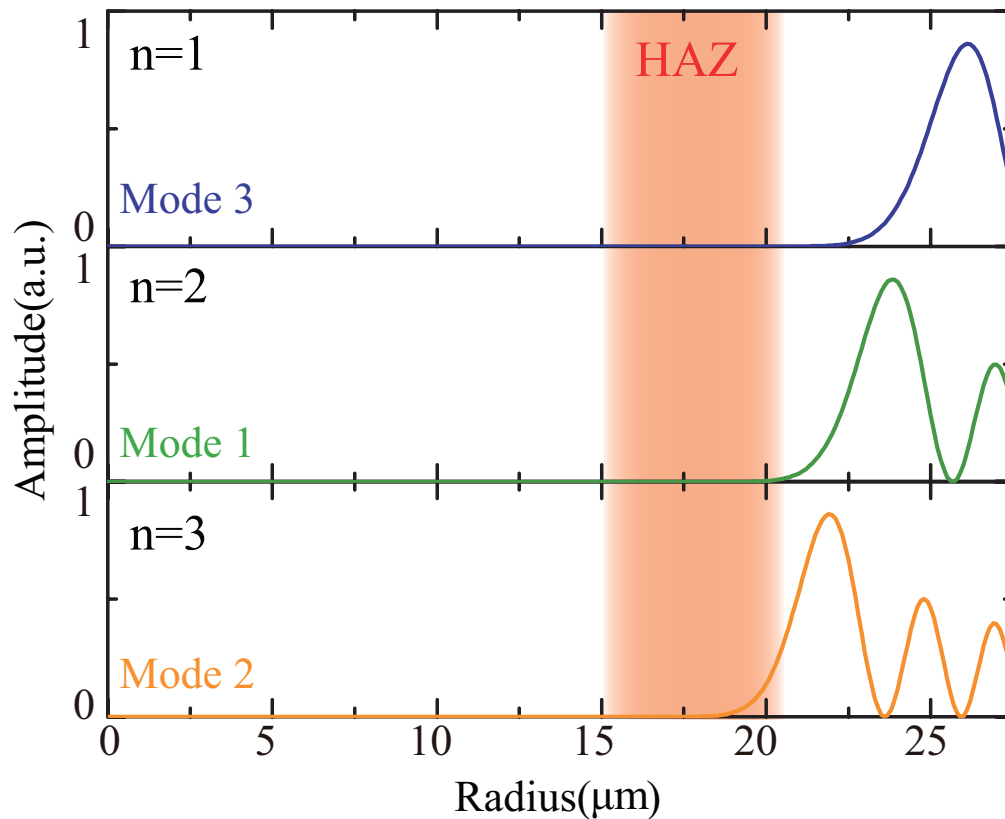


Fig. 5. Radial intensity distribution of mode 1, 2 and 3. The orange zone represents the heat affected zone induced by femtosecond laser shots. It has some overlapping with the intensity distribution of mode 2 resulting in a Q decrease.

by the defect created by the laser. The change in refractive index and micro structures of HAZ will have influence on the mode profile and decrease the Q factor. As for modes 3, the Q factor experiences a continuous increase for over one order of magnitude because of "light annealing". The "light annealing" process plays a role of precision surgery that it repairs some lattice disorders and periphery imperfections. Mode 3 is localized in the very edge as a result it won't be touched by the HAZ as can be seen in Fig.5. In addition, the debris ejected in the hole formation process has the least influence on it because most nano particles are in around of the hole. Furthermore it is the most sensitive mode to the periphery conditions. As a result, mode 3 experiences a significant increase.

When we further increase the irradiating laser power to 42mW we can see that all the other modes are disappeared and only mode 3 survived exhibiting relatively high Q factor, as is shown in Fig.6. The result further confirms that mode 3 is more localized in the periphery and as a result femtosecond laser HAZ and the ejected debris have the least influence on it. The inset is the COMSOL simulated mode profile. It clearly shows that it is the fundamental mode. For the effectiveness of the proposed method, we also inspected other LN microdisks by femtosecond laser irradiation. The modes localized in the most periphery ($n=1$) all exhibit different degrees of quality improvement.

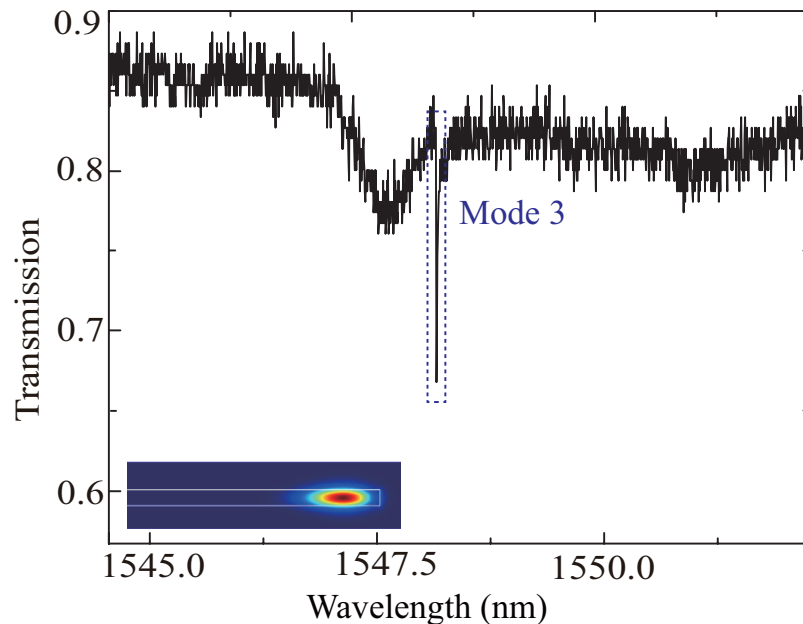


Fig. 6. Transmission spectrum after 42mW laser interaction. The inset shows the mode profile of mode 3.

4. Conclusion

In conclusion we have explored a new method to improve Q factor of the already-made micro-disk by femtosecond laser irradiation. The pulses confined in the edge of the disk will have compact nonlinear interaction with the lattices which may induce melting or resolidification process. Both of them will help rebuild the periphery and thus improve the quality. In addition high power laser shots may kill high order modes of the micro-disk leaving only fundamental modes. This method provides an access to work on a single component without touching other building blocks of an already fabricated chip. It may play a more and more important role in repairing impaired different building blocks and increasing device functionalities in future integrated photonic chips.

Funding

National Key R & D Program of China (2017YFA0303700); National Natural Science Foundation of China (NSFC) (11574208).

Acknowledgments

The device is fabricated at Center for Advanced Electronic Materials and Devices (AEMD).

References

1. G. Poberaj, H. Hu, W. Sohler, and P. Guenter, "Lithium niobate on insulator (Inoi) for micro-photonic devices," *Laser & Photonics Rev.* **6**, 488–503 (2012).
2. A. Boes, B. Corcoran, L. Chang, J. Bowers, and A. Mitchell, "Status and potential of lithium niobate on insulator (Inoi) for photonic integrated circuits," *Laser & Photonics Rev.* **12**, 1700256 (2018).
3. L. Cai, Y. Wang, and H. Hu, "Low-loss waveguides in a single-crystal lithium niobate thin film," *Opt. Lett.* **40**, 3013–3016 (2015).
4. L. Chang, Y. Li, N. Volet, L. Wang, J. Peters, and J. E. Bowers, "Thin film wavelength converters for photonic integrated circuits," *Optica* **3**, 531–535 (2016).

5. S. Liu, Y. Zheng, and X. Chen, "Cascading second-order nonlinear processes in a lithium niobate-on-insulator microdisk," *Opt. Lett.* **42**, 3626 (2017).
6. L. Ge, Y. Chen, H. Jiang, G. Li, B. Zhu, Y. Liu, and X. Chen, "Broadband quasi-phase matching in a mgo:ppln thin film," *Photon. Res.* **6**, 954–958 (2018).
7. S. F. Preble, Q. Xu, and M. Lipson, "Changing the colour of light in a silicon resonator," *Nat. Photonics* **1**, 293 (2007).
8. M. Wang, Y. Xu, Z. Fang, Y. Liao, P. Wang, W. Chu, L. Qiao, J. Lin, W. Fang, and Y. Cheng, "On-chip electro-optic tuning of a lithium niobate microresonator with integrated in-plane microelectrodes," *Opt. Express* **25**, 124–129 (2017).
9. T.-J. Wang, J.-Y. He, C.-A. Lee, and H. Niu, "High-quality LiNbO_3 microdisk resonators by undercut etching and surface tension reshaping," *Opt. Express* **20**, 28119–28124 (2012).
10. H. Jiang, H. Liang, R. Luo, X. Chen, Y. Chen, and Q. Lin, "Nonlinear frequency conversion in one dimensional lithium niobate photonic crystal nanocavities," *Appl. Phys. Lett.* **113**, 021104 (2018).
11. L. Chang, X. Jiang, S. Hua, C. Yang, J. Wen, L. Jiang, G. Li, G. Wang, and M. Xiao, "Parity-time symmetry and variable optical isolation in active-passive-coupled microresonators," *Nat. Photonics* **8**, 524–529 (2014).
12. N. Zhang, Z. Gu, S. Liu, Y. Wang, S. Wang, Z. Duan, W. Sun, Y. F. Xiao, S. Xiao, and Q. Song, "Far-field single nanoparticle detection and sizing," *Optica* **4**, 1151 (2017).
13. F. Lacour, N. Courjal, M.-P. Bernal, A. Sabac, C. Bainier, and M. Spajer, "Nanostructuring lithium niobate substrates by focused ion beam milling," *Opt. Mater.* **27**, 1421–1425 (2005).
14. C. Wang, M. J. Burek, Z. Lin, H. A. Atikian, V. Venkataraman, I.-C. Huang, P. Stark, and M. Lončar, "Integrated high quality factor lithium niobate microdisk resonators," *Opt. Express* **22**, 30924–30933 (2014).
15. J. Wang, F. Bo, S. Wan, W. Li, F. Gao, J. Li, G. Zhang, and J. Xu, "High-q lithium niobate microdisk resonators on a chip for efficient electro-optic modulation," *Opt. Express* **23**, 23072–23078 (2015).
16. J. Lin, Y. Xu, Z. Fang, M. Wang, J. Song, N. Wang, L. Qiao, W. Fang, and Y. Cheng, "Fabrication of high-q lithium niobate microresonators using femtosecond laser micromachining," *Sci. Reports* **5**, 8072 (2015).
17. B. Guha, F. Marsault, F. Cadiz, L. Morgenroth, V. Ulin, V. Berkovitz, A. Lemaître, C. Gomez, A. Amo, S. Combré *et al.*, "Surface-enhanced gallium arsenide photonic resonator with quality factor of 6×10^6 ," *Optica* **4**, 218–221 (2017).
18. D. Armani, T. Kippenberg, S. Spillane, and K. Vahala, "Ultra-high-q toroid microcavity on a chip," *Nature* **421**, 925 (2003).
19. M. Zhang, C. Wang, R. Cheng, A. Shams-Ansari, and M. Lončar, "Monolithic ultra-high-q lithium niobate microring resonator," *Optica* **4**, 1536–1537 (2017).
20. R. Wu, J. Zhang, N. Yao, W. Fang, L. Qiao, Z. Chai, J. Lin, and Y. Cheng, "Lithium niobate micro-disk resonators of quality factors above 10^7 ," *Opt. Lett.* **43**, 4116–4119 (2018).
21. D. Bachman, Z. Chen, R. Fedosejevs, Y. Y. Tsui, and V. Van, "Permanent fine tuning of silicon microring devices by femtosecond laser surface amorphization and ablation," *Opt. Express* **21**, 11048–11056 (2013).
22. D. Bachman, Z. Chen, R. Fedosejevs, Y. Tsui, and V. Van, "Threshold for permanent refractive index change in crystalline silicon by femtosecond laser irradiation," *Appl. Phys. Lett.* **109**, 091901 (2016).
23. A. H. Nejadmalayeri and P. R. Herman, "Rapid thermal annealing in high repetition rate ultrafast laser waveguide writing in lithium niobate," *Opt. Express* **15**, 10842–10854 (2007).
24. S. Liu, W. Sun, Y. Wang, X. Yu, K. Xu, Y. Huang, S. Xiao, and Q. Song, "End-fire injection of light into high-q silicon microdisks," *Optica* **5**, 612–616 (2018).
25. X. Jiang, L. Shao, S.-X. Zhang, X. Yi, J. Wiersig, L. Wang, Q. Gong, M. Lončar, L. Yang, and Y.-F. Xiao, "Chaos-assisted broadband momentum transformation in optical microresonators," *Science* **358**, 344–347 (2017).
26. L. Wang, C. Wang, J. Wang, F. Bo, M. Zhang, Q. Gong, M. Lončar, and Y.-F. Xiao, "High-q chaotic lithium niobate microdisk cavity," *Opt. Lett.* **43**, 2917–2920 (2018).
27. R. R. Gattass and E. Mazur, "Femtosecond laser micromachining in transparent materials," *Nat. Photonics* **2**, 219 (2008).
28. M. Garcia-Lechuga, J. Solis, and J. Siegel, "Melt front propagation in dielectrics upon femtosecond laser irradiation: Formation dynamics of a heat-affected layer," *Appl. Phys. Lett.* **108**, 171901 (2016).
29. T. Seuthe, A. Mermillod-Blondin, M. Grehn, J. Bonse, L. Wondraczek, and M. Eberstein, "Structural relaxation phenomena in silicate glasses modified by irradiation with femtosecond laser pulses," *Sci. Reports* **7**, 43815 (2017).
30. J. Bonse, S. Wiggins, and J. Solis, "Dynamics of femtosecond laser-induced melting and amorphization of indium phosphide," *J. applied physics* **96**, 2352–2358 (2004).